Experimental Investigation of combustion characteristics, Performance, and emission of a Spark Ignition Engine with 2nd Generation bio-gasoline and ethanol fuels

Mohamed M, Zhao H, Harrington A and Hall J ,

Abstract

Climate change mitigation is the main challenge for the automotive industry, as the government issues legislation to combat CO2 emissions. In addition to electrification and battery electric vehicles, using low carbon and zero carbon fuels in Internal Combustion (IC) engines can also be an effective way to reach net zero carbon transport.

This study investigated and compared the combustion characteristics, performance and emissions of a highly boosted spark ignition (SI) engine fuelled with EU VI 95RON E10 gasoline and blends of second-generation bio-gasoline with different ethanol contents of 5% (E5), 10% (E10), and 20% (E20). The single-cylinder SI engine was equipped with a centrally mounted high-pressure injector and supplied externally boosted air. Engine experiments were conducted at 2000RPM and 3000RPM with low and high load operations.

The overall finding indicates that increasing the ethanol content of second-generation biofuels from 5% to 20% improves the indicated thermal efficiency at low load by 2.1% and increases the knock resistance by 16.8% at high load operation as well as a reduction by 0.7% on cycle-to-cycle variation. The engine emissions were primarily affected by the engine operating conditions, and no consistent correlation between the ethanol content and emissions. However, it was noted that the average NOx and THC emissions were increased by 11.02% and 66%, respectively, at the low load operation when the ethanol content was increased from 5% to 20% at the exact fuel injection timing of 350 BTDC.

1. Introduction

The powertrain technology used in every transportation sector must be significantly changed to achieve the worldwide goal of a zero-carbon society.

In order to transition toward a net carbon zero society in 2050 and beyond, significant efforts are being made by the automotive industry to reduce and eliminate carbon emissions from the vehicles on the road. CNG (compressed natural gas) has been introduced as an alternative low carbon fuel [5], but the infrastructure for using natural gas as a transportation fuel is not as developed as liquid fuels. Thus, Alcoholic fuels are introduced worldwide as excellent fossil fuel replacements in the form of blended fuel with the fossil fuel. This contrasts with other alternative fuels that require extensive infrastructure and fleet upgrades[15][16][17]. As a result, immediate and significant impact can be achieved on the reduction in carbon emissions both in the tailpipe and the life-cycle of the fuel and vehicle usage. On the other hand, Increasing oxygenated fuel percentages with fossil fuels produces some challenges, such as the cold start issues with higher ethanol concentrations [6][7][8][9][10]. Overall, premixed alcohol/gasoline fuels show a significant drop in the total emission of the vehicle with less particulate number; however, some emission parameters, such as the NOx emission, have a different response on SI engines depending on the powertrain setup itself [11][12].

Previous studies also show that ethanol and methanol outperform gasoline engines with higher thermal efficiency in most operating conditions. The increase in the thermal efficiency is more pronounced at higher loads and power outputs. The strong knock resistance of ethanol and methanol permits more advanced combustion phasing, eliminating the need for over-fueling under full load and power operations. This is because the higher latent heat and lower air-fuel ratio of alcohol fuels contribute to a higher knock resistance [13] [14].

In addition to the use of bio-ethanol, bio-gasoline can be produced and used. Modern bio-derived gasoline fuels have been tested using a steady-state engine dynamometer and a transient vehicle test with a mandated driving cycle. The findings demonstrate that such fuels can be utilised as a drop-in substitute for normal gasoline fuel produced from fossil sources without requiring any engine adjustments or change in the fueling system [18].

This study aims to investigate the performance and emission performance of a spark-ignited (SI) engine operated with the bio-gasoline with three different concentrations of ethanol, E5, E10, and E20, all with a RON value of 95. The first set of experiments were carried out at various load points at a constant engine speed of 3000 RPM. The combustion characteristics, engine performance and emissions measured using the same fuel injection parameters as those used in the baseline gasoline fuel. Then, the combustion, efficiency and emissions of three blended biofuels were evaluated at multiple parts- and high-load operating conditions with different injection parameters.

2. Experimental setup

The single cylinder is constructed with a single cylinder engine block and a cylinder head from a Mahle 3-cylinder highly-downsized gasoline engine. It is mounted on a fully instrumented AC dynamometer testbed as shown in Figure 1. The versatility and adaptability of single-cylinder engine testing helps to reduce engine development time, expense, and complication in the engine control unit.

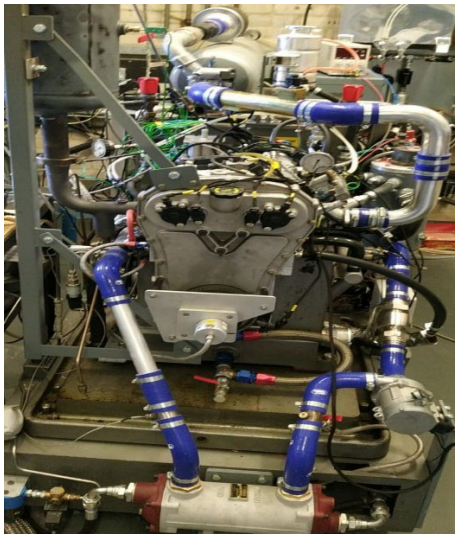

Figure 2. Picture of the single-cylinder engine testbed at Brunel University.

Prior work on this single-cylinder research engine involved a combination of port fuel injection (PFI) and direct injection (DI) and an evaluation of water injection. The engine has been since modified with a centrally-located solenoid GDI injector for operation on pure DI ethanol and methanol [14][22][23].

Table 1 displays the hardware specifications for the engine. The cylinder head includes two intake valves, two exhaust valves, and double overhead camshafts with hydraulically changeable cam phasers capable of 40°CA. The centrally-mounted direct injector can operate at pressures as high as 200 bar. The ignition system's spark plug is also positioned centrally with a 100 mJ coil-on-plug configuration. Lastly, the engine is managed by a MAHLE Versatile ECU (MFE), which employs a control software framework that is adaptable to any new engine technology and is flexible and easily customisable.

Table 1. Specification of the Single-Cylinder Engine.

Configuration	Single Cylinder
Displaced volume	400 cc
Stroke	73.9 mm
Bore	83 mm
Geometric Compression Ratio	11.1: 1
Number of Valves	4
Exhaust Valve Timing	EMOP (Exhaust Maximum Opening Point) 100-140°CA BTDC, 11 mm Lift, 278°CA Duration
Inlet Valve Timing	IMOP (Intake Maximum Opening Point) 80-120°CA ATDC, 11 mm Lift, 240°CA
Injection System	Central Direct Injection outwardly opening spray ≤200
Injection Control	MAHLE Flexible ECU (MFE)

Figure 2 illustrates the arrangement of the testbed, which includes an external boosting system that is operated separately. The intake and exhaust pressures were measured by two high-speed piezo-resistive pressure sensors. In addition, the coolant and oil temperatures were controlled to ensure stable and consistent coolant temperatures for the steady-state testing conducted under all conditions in which the engine operates. Gaseous emissions were measured using a HORIBA (MEXA-554JE for CO/CO_2) and Signal analysers (Ambitech model 443 Chemiluminescent NO/NOx and Rotork Analysis model 523 flame ionisation detection (FID) hydrocarbon (HC) analysers). A Cambustion DMS500, capable of measuring the particle size distribution, was used to quantify the particle emissions [24].

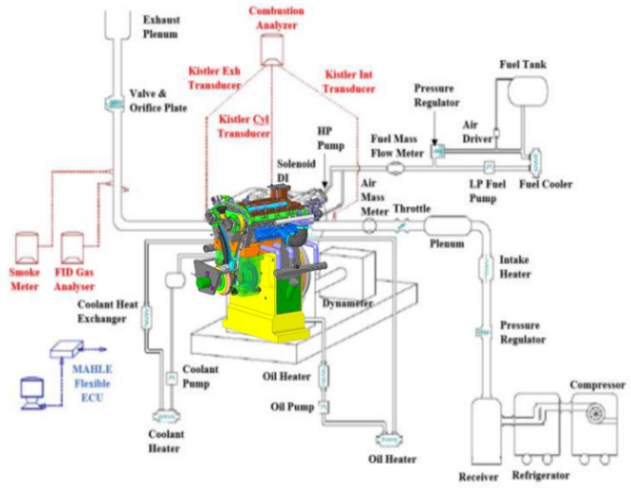

Figure 2. Testbed Layout.

The test cell is fitted with a Data Acquision system comprising a NI-USB 6353 fast card capable of having 32 analog inputs at a speed of 1.25 MS/s and a NI-USB 6210 card as an extra time domain card. This system can capture all data in the crank domain as well as the time domain to conduct quick analyses and can also accept additional input from pressure and temperature sensors the time domain. An in-house combustion analyses programme was used to generate live monitoring of the primary combustion parameters, and record the in-cylinder pressure data up to 300 cycles.

3. Biofuel properties

This study used a bio gasoline fuel that was produced via a two-step process . The first step is to produce bioethanol from waste biomass, or agricultural waste such as straw. This lignocellulosic biomass is initially pretreated to increase enzyme accessibility. After pretreatment, the biomass is subjected to enzymatic hydrolysis to convert it into sugars, which are then fermented to ethanol using a mixture of microorganisms. This bio-ethanol is then dehydrated into ethylene and "grown" at 300-400 °C in the presence of a zeolite catalyst into longer chain hydrocarbons, as shown in Figure 3 [25].

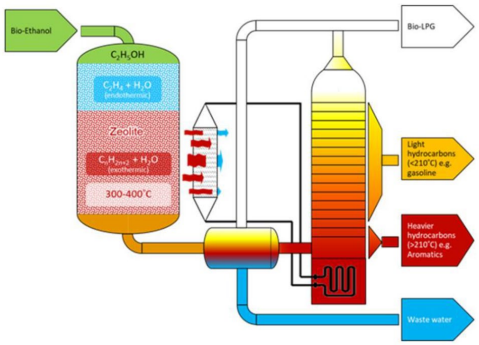

Figure 3. Schematic of the ethanol-to-gasoline conversion process [26].

The specifications of the testing fuels are givn in Table 2. The baseline gasoline is not only compliant with the EN228 fuel standard, which may cover a vast range of fuel performance, but also has a very high specification, including a low particle index, made possible by a complex mixing. This fuel standard was chosen as a demanding benchmark for bio-gasoline fuels. Blended bio-fuels with the same octane rating but varying ethanol concentrations were prepared and studied.

Table 2. Fuels properties used in the experimental study.

Parameter	Unit	Fossil 95 E10	Bio E5	Bio E10	Bio E20
Bio-Content	% v/v	-	82.9	100	100
Honda Particulate Mass Index		1.03	2.17	2.25	1.88
Simplified Particulate Mass Index		-	2.15	2.49	-2.95
R.O.N.		95.50	95.20	95.90	96.20
M.O.N.		85.10	85.10	84.60	85.00
Carbon	% (m/m)	83.06	84.77	83.10	79.02
Hydrogen	% (m/m)	13.35	13.44	13.31	13.57
Density at 15°C	kg/L	0.753	0.752	0.763	0.761
Initial Boiling Point	°C	34.9	30.1	30.1	34.9
H/C Ratio		1.915	1.889	1.908	2.046
O/C Ratio		0.03244	0.01585	0.03243	0.07039
AFR (Stoic)	assume s	14.66	14.63	14.65	14.85
AFR (Stoic)	assume s	13.98	14.29	13.97	13.43
Percentage H+C+O	%	100.00	100.00	100.00	100.00
Ethanol & Higher Alcohols	% (v/v)	9.8	4.9	10	20.4
Net Calorific value **(LHV)**	MJ/kg	41.33	41.91	40.98	39.36
Gross Calorific value	MJ/kg	44.17	44.76	43.8	42.23
Sulfur Content	mg/kg	3.2	<1	<1	<1

Figure 4 shows that the fossil gasoline had a lighter composition than the studied bio-gasolines since a more significant proportion of the fuel evaporated at lower temperatures. This is a product of the bio-feedstock gasoline and the manufacturing process. Typically, high-grade fossil gasoline undergoes further processing to eliminate aromatic components to decrease the creation of hazardous particles during burning.

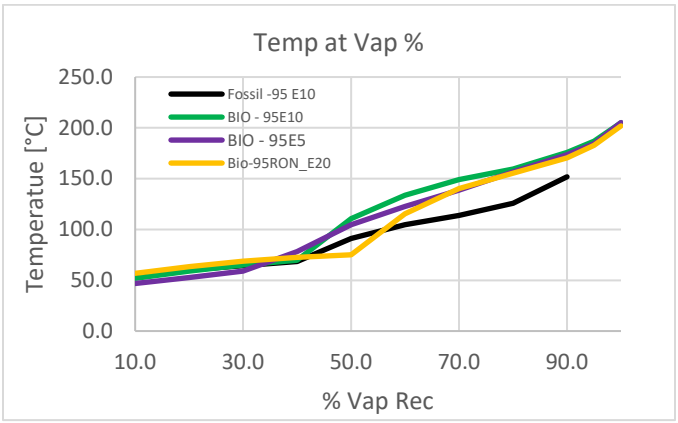

Figure 4. Fuel evaporation characteristics for all fuels analysed.

Figure 5 shows each chemical contents of the bio fuels which have been adjusted to keep the RON number equal with different ethanol percentages. Components with a high molecular weight result in a fuel with a higher boiling point, which tends to produce more soot particles and increased chance of wall wetting. The resulting fuel-oil combination has a more significant potential of leaving the combustion chamber in droplet form, contributing to the emission and combustion performance[27].

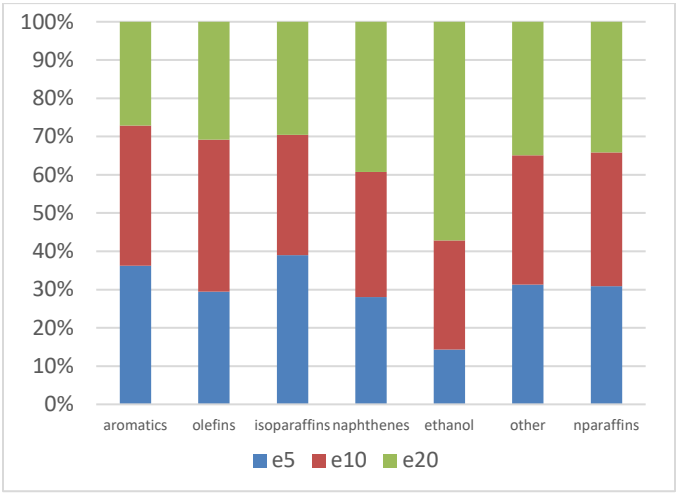

Figure 5. Biofuels compositions.

4. Test methodology

The single-cylinder engine tests were carried out at 3000 RPM because of its relative high occupancy over a drive cycle range. The differences in performance and emissions were analyzed of bio fuels compared to the baseline gasoline at different loads. The load sweeps were conducted with consistent engine settings (e.g., cam timing, fuel injection pressure and timing) to remove any comparability variation.

In the second part of the study, effects of fuel injection pressure and start of fuel injection timings were investigated for the Therefore,

Moving to the low and high load fuel matrix tests for an in-depth comparison between the three biofuels to analyse the effect of higher ethanol content and assess the performance profile of each biogasoline over wide injection angles and different injection pressures. Finally, analyse the emission over the vast operation regime to study the effect of the ethanol increase over the vast operation points.

5. Test results and discussion

water and oil temperatures were kept constant at 90ºC, and the Intake air temperature was at 40ºC with zero per cent humidity. Three sets of experiments were carried out. Firstly, results will be presented and discussed for the 95 RON E10 baseline gasoline and biogasoline with different ethanol concentrations at 3000 rpm and varying load sweep from 2bar to 28bar IMEP. The same fuel injection pressure and initial injection timings optimised for the baseline gasoline were used for all the tested fuels.

The second experiment was carried out at 4.6 bar IMEP in 2000rpm to investigate the effect of injection parameters on the biogasoline fuels with different ethanol content at low load engine operation. The third experiment was carried out at 16 bar IMEP and 3000rpm to study the effect of injection parameters on engine performance and emissions at high power operation.

5.1 Effect of fuel composition on combustion, efficiency and emissions at different loads with the same fuel injection parameters

In this test, the engine speed was fixed at 3000RPM, and the load varied from 2 bar IMEP to 28 bar IMEP. The engine operating parameters, including the rail pressure, the start of injection time, and the intake and exhaust valve timings, were kept the same at each operating condition for different fuels, and they were determined for optimised engine performance in the baseline tests with gasoline. It is noted that the end of injection was delayed with the increase in ethanol content due to more fuel in volume to be injected.

In most conditions, the engine was operated with stoichiometric combustion by measuring the relative air-to-fuel ratio using a Lambda sensor in the exhaust. However, above 24 bar IMEP, as shown in Figure 7, the lambda value was reduced to 0.9 to keep the exhaust temperature below 750ºC.

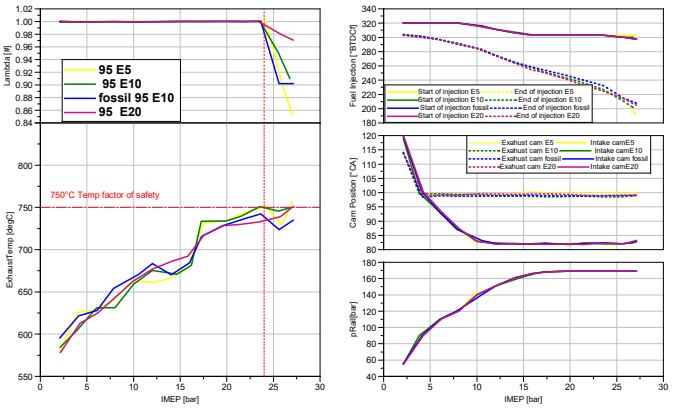

Figure 7. 3000 RPM load sweep data shows the lambda value, Exhaust temperature, fuel injection angle, cam timing, and fuel rail pressure.

As shown in Figure 8, the knock intensity, defined as abnormal and stochastic combustion phenomenon that limits the efficiency of the spark ignition engine, increased steadily as the engine load was increased and reached its peak at 20 bar IMEP. As the load was changed from 2-14 bar IMEP, the burn durations measured by the spark to 10%, 10 to 50%, and 50- 90% mass fraction burned were reduced to a minimum because faster combustion at elevated gas pressure and temperature. Consequently, the spark timing was retarded, and the MBT could be reached. Above 15 bar IMEP, the spark timing had to be retarded beyond the MBT to keep the knock intensity below 1.0. This resulted in slower combustion and extended burn durations.

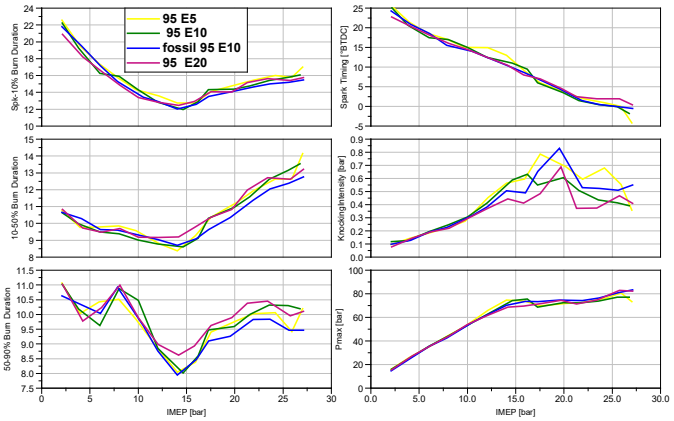

Figure 8. 3000 RPM load sweep data shows spark-to-10% MFB duration, 10-90% MFB durations, spark timing, Knoicking intensity, and Incylinder pressure.

Concerning the effect of fuel properties, it is noted that baseline gasoline and blends of bio-gasoline and ethanol exhibited similar combustion characteristics at part-load up to 12bar IMEP when the wide-open-throttle (WOT) condition was reached. As the load was increased further, the addition of ethanol caused increased combustion durations but lower knock intensity when the engine was operated with boosted air.

At the highest load of 25bar IMEP, less fuel enrichment was needed to keep the exhaust gas temperature below the limit of 750º (Figure 7) and hence higher combustion efficiency shown in Figure 8.

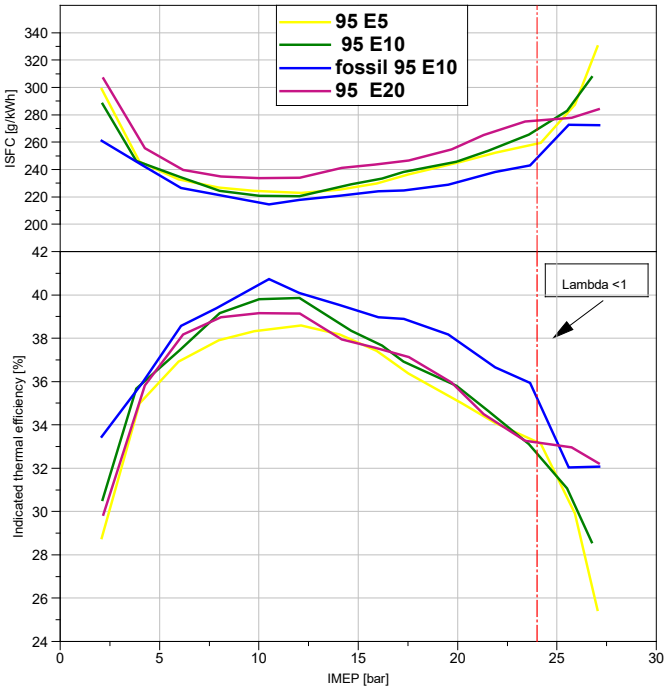

Figure 9. 3000 RPM load sweep data shows The indicated specific consumption and the ITE.

Figure 9 shows the indicated specific consumption and engine thermal efficiency as a function of load for different fuel blends. It can be seen that the gasoline fuel produced higher engine efficiency and lower specific fuel consumption when the same fuel injection parameters and spark timings were used.

Finally, Figure 10 shows the corresponding engine out emissions for different fuel blends at a load function. The increased CO and HC emissions at the highest load conditions were attributed to the fuel-rich combustion. The CO emission was inversely proportional to the lamda value, and the E20 biogasoline produced the lowest CO emission at the highest load. Higher HC emission was observed with biogasoline fuel blends thanks to the higher content of heavy hydrocarbons in bio-gasoline.

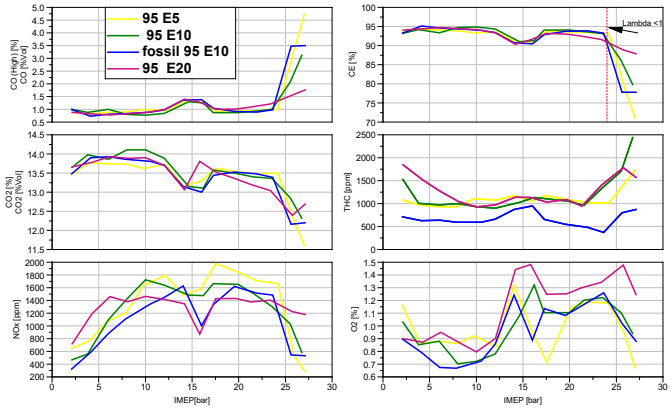

Figure 10. 3000 RPM load sweep data shows the emission captured.

The above results showed that less fuel enrichment was needed, and hence lower emissions could be achieved at the highest load with biogasoline with higher ethanol content. However, lower engine efficiencies were obtained from biogasoline and ethanol blends if the fuel injection parameters optimised for gasoline were used.

Finally, figure 11 shows the Pm emission captured by DMS 500, which shows the numbers of particulate matter over the load, which shows higher numbers for the biofuels than the fossil fuel due to the haver compositions of the biofuels which can be reduced by adding PM filter.

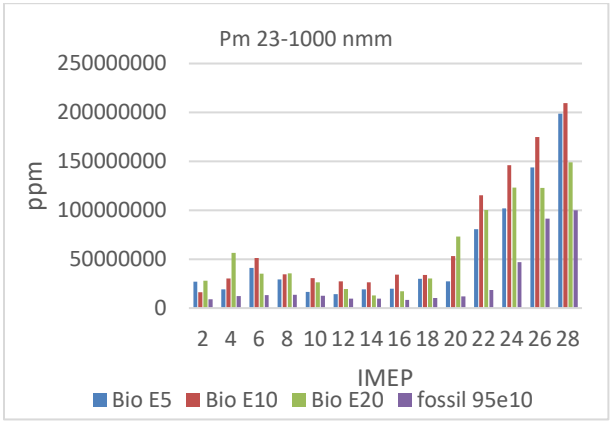

Figure 11. 3000 RPM load sweep data shows the Pm numbers for 23-1000 nmm size.

Therefore, it was decided to carry out additional experiments to see if the engine thermal efficiency of biogasoline and ethanol blends could be improved by optimising the fuel injection parameters at low and high load operations.

5.2 Effect of Fuel injection parameters on combustion, efficiency and emissions of bio gasoline fuels at low load engine operation

This test aims to investigate the effect of fuel injection pressure and the start of fuel injection for optimised engine operations with different bio gasoline and ethanol blends at a low load engine operation of 2.4 bar IMEP and 2000 RPM engine speed. The start of the injection timing was varied from 275 ca BTDCf to 350ca BTDCf at 25 degrees interval. The fuel injection pressure was increased from 50 bar to 200 bar with a 50 bar step. Figure 12 shows the combustion phasing and comustion duration results as a function of fuel injection pressure (y-axis) and the start of injection timing (x-axis). As the spark timings were set to MBT, the combustion phasing as indicated by 50% MFB remained constant at 8ca ATDC. It is noted that there was little change in the combustion duration for a given start of fuel injection whilst the most prolonged burn duration occurred at 300ca BTDCf irrespective of the injection pressure and independent of the ethanol content.

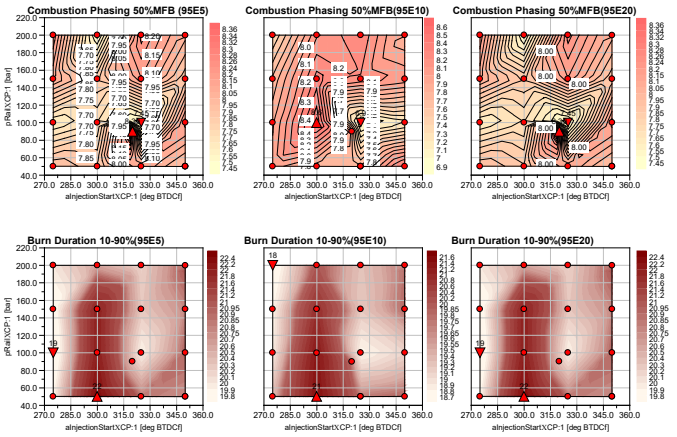

Figure 12. 2000 RPM fuel Matrix data shows combustion phasing and the Burn duration.

The results in Figure 13 show that the maximum indicated thermal efficiency increased slightly with more ethanol, but the ISFC increased at the lowest thermal efficiency area, thanks to the lower calorific value of ethanol. Moreover, looking at the thermal efficiency distribution, both bio-gasoline E20 and E10 achieved the maximum efficiency at 325ca BTDCf and 100 bar injection pressure. In contrast, E5 fuel obtained a higher thermal efficiency at the late injection timing and higher injection pressure. Overall, the variation of the thermal efficiency was within 1% when the fuel injection pressure and start injection timings were changed significantly.

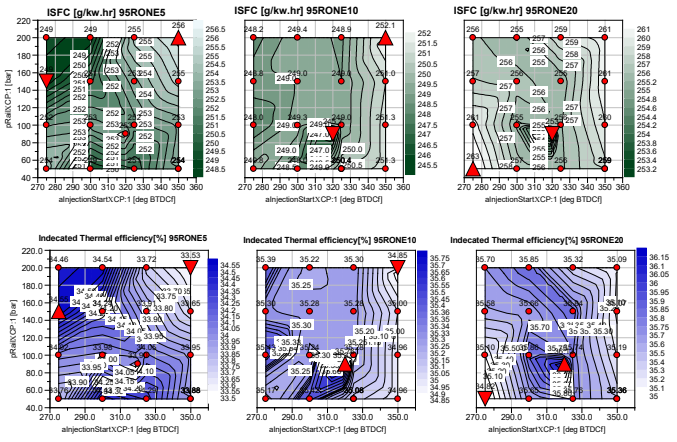

Figure 13. 2000 RPM fuel Matrix data shows ISFC and ITE.

Figure 14 shows distributions of the THC and NOx emissions as a function of fuel injection pressure and the start of injection. At the same injection pressure and timing, the THC emission increased slightly with the percentage of ethanol, probably because of the longer injection duration and delayed injection end, leading to less homogeneous mixtures. For each fuel, the minimum HC emissions were obtained with the start of fuel injection at 325ca BTDCf. Too early injection would lead to more fuel trapped in the crevices, and too late injection caused incomplete fuel evaporation and even fuel spray impingement on the piston top. At this part-load and low-speed engine operation, the fuel injection pressure had little effect on the HC emissions.

It is also noted that the lowest NOx emission was obtained with E20 with the most retarded injection timing and lower injection pressure due to the lower combustion temperature of E20 and slightly retarded combustion.

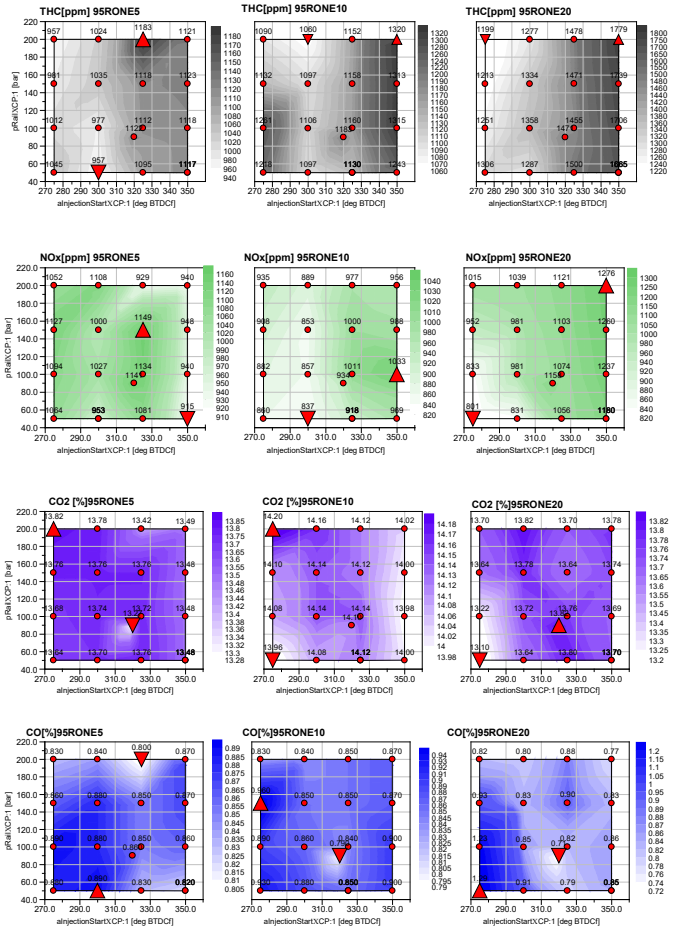

Figure 14. 2000 RPM fuel Matrix data shows Emission data.

5.3 Effect of Fuel injection parameters on combustion, efficiency and emissions of bio gasoline fuels at high power engine operation

This test aims to analyse the effect of fuel injection parameters on the three bio gasoline and ethanol blends at a the high power engine operation. The test consisted of 18 testing points with stoichiometric combustion at a fixed speed of 3000 RPM at 16bar IMEP.

Due to occurrence of knocking combustion at such a high load with intake pressure at 1.3bar, the spark timing was retarded and the combustion stability became a potential issue when more combustion took place well after TDC. Thus, the combustion stability as measure by the CoV (%) in IMEP was measured and analysed as shown in Figure 15.

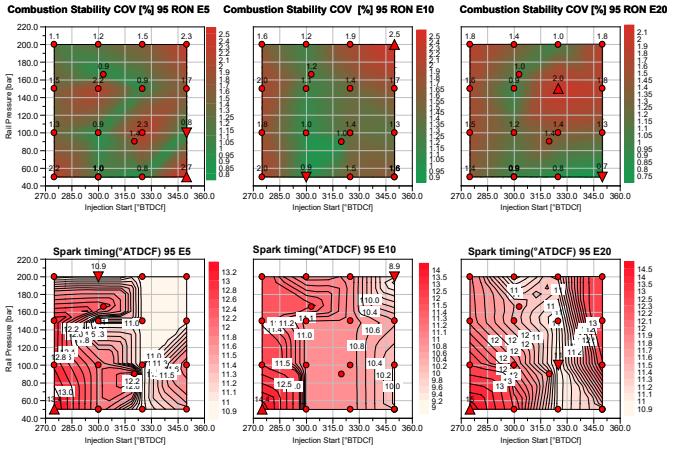

Figure 15. 3000 RPM fuel Matrix data shows combustion stability and spark timing.

The results show that E20 fuel was characterised by more stable combustion with lower CoV, and the most stable combustion was obtained with the start of fuel injection at around 300 ca BTDCf for all three fuels. There was no consistent trend in the change of combustion stability with injection pressure and injection timing, except for E20, which had lower CoV values at the lower injection pressure.

The combustion phasing and the burn duration results are shown in Figure 16.

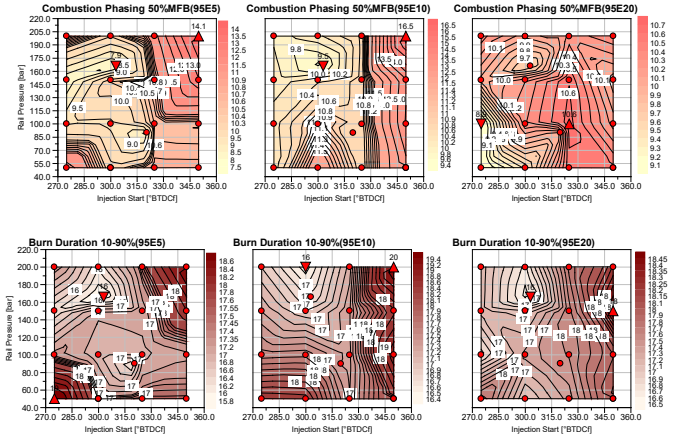

Figure 16. 3000 RPM fuel Matrix data shows combustion phasing and the Burn duration.

The combustion phasing at 50% MFB shows less deviation for E20 fuel than for E5 and E10. Also, the most retarded combustion was obtained with the earliest injection angle of 350ca BTDCf at higher injection pressures. The burn duration results show a similar trend for the three biofuels. When the combustion was most stable, the minimum burn duration was obtained with 300ca BTDCf injection timing.

As shown in Figure 17, the highest indicated thermal efficiency was obtained with the highest injection pressure and the start of injection timing of 300 ca BTDCf for all three fuels. As the fuel injection took place earlier, the thermal efficiency decreased steadily, which was in line with the increased HC emissions shown in Figure ??. As the ethanol content was increased, the thermal efficiencies were increased slightly across the range of injection pressures and injection timings tested. As expected, the fuel consumption increased with more ethanol added due to the lower net calorific value of the higher ethanol content biofuels.

The injection timing and pressure had a more apparent impact on the thermal efficiency than the low load operation. The variation was about 6%, much higher than the 4.6 bar IMEP.

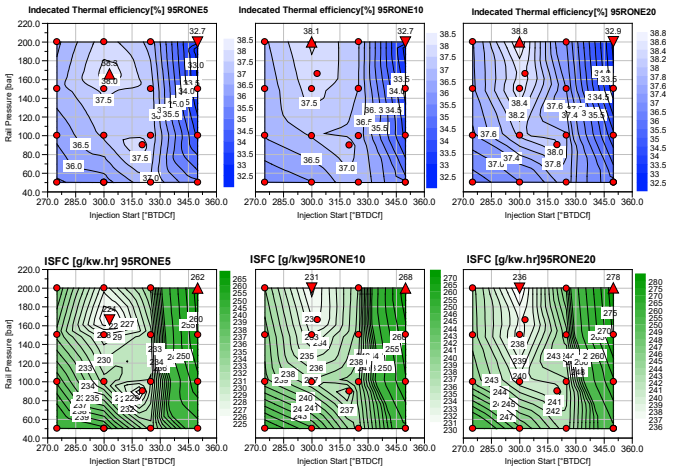

Figure 17. 3000 RPM fuel Matrix data shows ITE and ISFC.

The unburnt HC emissions of all three fuels reached their minima with the start of injection at 300 ca BTDC and 200 bar injection pressure. The THC increased with higher ethanol fuel and the highest HC emissions were obtained with the earliest injection timing because of more trapped fuel in crevices as shown in the figure 18.

The NOx emissions increased with ethanol percentages, because of more advanced spark timing.

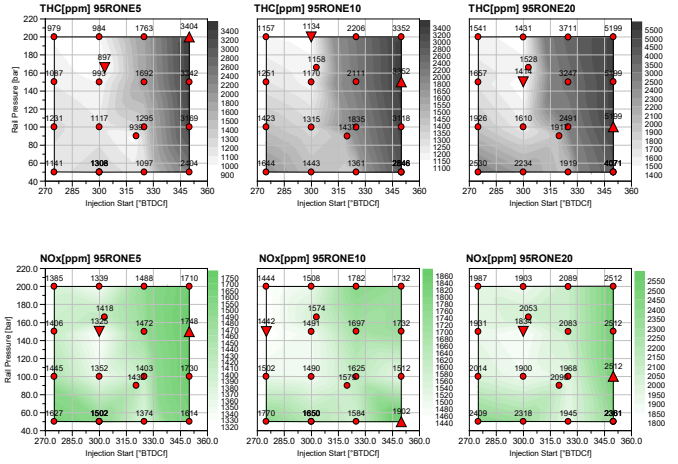

Figure 18. 3000 RPM fuel Matrix data shows THC and Nox emissions.

As shown in Figure 19, the carbon monoxide emission increased with retarded injection timing because of the fuel-rich mixture formed by the incomplete mixing from the reduced time for mixture formation and probably the increased impingement of fuel onto the piston top. The total CO variation is less than 0.5%. E20 produced the lowest CO

emission as it had the lowest carbon content, and the CO_2 emissions remained almost constant at around 13%.

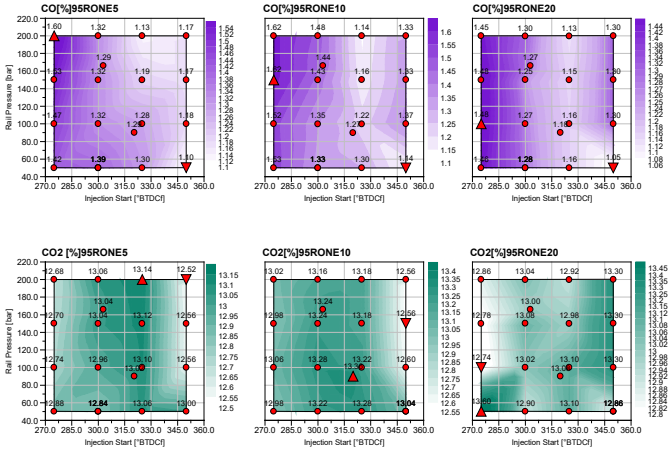

Figure 19. 3000 RPM fuel Matrix data shows carbon monoxide and dioxide emissions.

Summary and Conclusions

In this study, three sets of experiments were carried out to investigate the biogasoline and its blend with ethanol in a single-cylinder spark ignition engine. Both the effects of fuel properties and fuel injection parameters were measured and analysed on the combustion process, thermal efficiency, and emissions. The main findings can be summarised as follows.

At 3000rpm and loads from 2 bar to 12bar IMEP, the 95 RON E10 baseline gasoline, blends of bio-gasoline, and ethanol exhibited similar combustion characteristics when the engine was operated with the natural aspiration with intake pressure below 1 bar. Less fuel enrichment was needed; hence, lower emissions could be achieved at the highest load with biogasoline E20. However, slightly lower engine efficiencies were obtained from biogasoline and ethanol blends when the fuel injection parameters optimised for gasoline were used.

At the low load operation of 4 bar IMEP at 2000rpm, the combustion duration remained constant as the injection pressure was increased from 50 bar to 200 bar for a given start of fuel injection, whilst the most prolonged burn duration occurred at 300ca BTDCf irrespective of the injection pressure and independent of the ethanol content. That maximum indicated thermal efficiency increased slightly. Overall, the variation of the thermal efficiency was within 1% when the fuel injection pressure and start injection timings were varied.

When the engine was operated at the high load of 16 bar IMEP at 3000rpm, the injection timing and pressure effect had a more apparent impact on the thermal efficiency at the high load operation than the low load operation. The variation was about 6%, much higher than the 4.6 bar IMEP. It is noted that E20 was the most knock resistant and exhibited more stable combustion. For all three fuels tested, the most stable combustion was obtained with the start of fuel injection at around 300 ca BTDCf, but there was no consistent trend in the change of combustion stability with injection pressure. The burn duration results show a similar trend for the three biofuels. When the combustion was most stable, the minimum burn duration was obtained with 300ca BTDCf injection timing. As the ethanol content was increased, the thermal efficiencies were increased slightly across the range of injection pressures and injection timings tested.

References

[1] I. E. Agency, “The Contribution of Natural Gas Vehicles to Sustainable Transport WO R K I N G PA P E R,” 2010.

[6] T. L. Alleman, “Analysis of Ethanol Fuel Blends,” *SAE Int. J. Fuels Lubr.*, vol. 6, no. 3, pp. 870–876, Nov. 2013, doi: 10.4271/2013-01-9071.

[7] R. A. Stein, J. E. Anderson, and T. J. Wallington, “An Overview of the Effects of Ethanol-Gasoline Blends on SI Engine Performance, Fuel Efficiency, and Emissions,” *Int. J. Engines*, vol. 6, no. 1, pp. 470–487, 2013, doi: 10.2307/26277631.

[8] T. Cavalcante Cordeiro de Melo *et al.*, “In Cylinder Pressure Curve and Combustion Parameters Variability with Ethanol Addition,” 2012.

[9] Y. L. Calvin *et al.*, “Volatility and physicochemical properties of gasoline-ethanol blends with gasoline RON-based 88, 90, and 92,” *Fuel*, vol. 307, no. July 2021, p. 121850, 2022, doi: 10.1016/j.fuel.2021.121850.

[10] A. Kumar, D. S. Khatri, and M. K. G. Babu, “An Investigation of Potential and Challenges with Higher Ethanol-gasoline Blend on a Single Cylinder Spark Ignition Research Engine,” 2009, [Online]. Available: http://www.sae.org.

[11] P. Iodice, A. Amoresano, and G. Langella, “A review on the effects of ethanol/gasoline fuel blends on NOX emissions in spark-ignition engines,” *Biofuel Res. J.*, vol. 8, no. 4, pp. 1465–1480, Dec. 2021, doi: 10.18331/BRJ2021.8.4.2.

[12] B. M. Masum, H. H. Masjuki, M. A. Kalam, I. M. Rizwanul Fattah, S. M Palash, and M. J. Abedin, "Effect of ethanol-gasoline blend on NOx emission in SI engine," *Renewable and Sustainable Energy Reviews*, vol. 24. pp. 209–222, 2013, doi: 10.1016/j.rser.2013.03.046.

[13] S. Verhelst, J. W. Turner, L. Sileghem, and J. Vancoillie, "Methanol as a fuel for internal combustion engines," *Progress in Energy and Combustion Science*, vol. 70. Elsevier Ltd, pp. 43–88, Jan. 01, 2019, doi: 10.1016/j.pecs.2018.10.001.

[14] A. Harrington, J. Hall, M. Bassett, E. Lu, and H. Zhao, "Combustion Characteristics and Exhaust Emissions of a Direct Injection SI Engine with Pure Ethanol and Methanol in Comparison to Gasoline," *SAE Tech. Pap. Ser.*, vol. 1, 2022, doi: 10.4271/2022-01-1089.

[15] T. Larsson, O. Stenlaas, and A. Erlandsson, "Future Fuels for DISI Engines: A Review on Oxygenated, Liquid Biofuels," in *SAE Technical Papers*, Jan. 2019, vol. 2019-January, no. January, doi: 10.4271/2019-01-0036.

[16] B. Morey, *Future Automotive Fuels and Energy*. 2013.

[17] M. Thewes, M. Müther, A. Brassat, S. Pischinger, and A. Sehr, "Analysis of the Effect of Bio-Fuels on the Combustion in a Downsized DI SI Engine," 2011.

[18] A. Harrington *et al.*, "Technical Assessment of the Feasibility of the use of Bio-Gasoline as a Drop-In Gasoline Fossil Fuel Replacement," *SAE Tech. Pap. Ser.*, vol. 1, pp. 1–12, 2022, doi: 10.4271/2022-01-1087.

[19] D. Hancock, N. Fraser, M. Jeremy, R. Sykes, and H. Blaxill, "A new 3 cylinder 1.2l advanced downsizing technology demonstrator engine," *SAE Tech. Pap.*, vol. 2008, no. 724, pp. 776–790, 2008, doi: 10.4271/2008-01-0611.

[20] M. J. Atkins and C. R. Koch, "A Well-to-Wheel Comparison of Several Powertrain Technologies," vol. 2003, no. 724, 2022.

[21] M. Bassett *et al.*, "Heavily Downsized Gasoline Demonstrator," *SAE Int. J. Engines*, vol. 9, no. 2, pp. 729–738, 2016, doi: 10.4271/2016-01-0663.

[22] R. Golzari, Y. Li, and H. Zhao, "Impact of Port Fuel Injection and In-Cylinder Fuel Injection Strategies on Gasoline Engine Emissions and Fuel Economy," no. Di, 2016, doi: 10.4271/2016-01-2174.Copyright.

[23] R. Golzari, H. Zhao, J. Hall, M. Bassett, J. Williams, and R. Pearson, "Impact of intake port injection of water on boosted downsized gasoline direct injection engine combustion , efficiency and emissions," vol. 22, no. 1, pp. 295–315, 2021, doi: 10.1177/1468087419832791.

[24] P. Price, B. Twiney, R. Stone, K. Kar, and H. Walmsley, "Particulate and hydrocarbon emissions from a spray guided direct injection spark ignition engine with oxygenate fuel blends," *SAE Tech. Pap.*, no. x, 2007, doi: 10.4271/2007-01-0472.

[25] "Are biofuels and e-fuels the only sustainable solution to power our existing fleet of internal combustion engines? - Coryton." https://coryton.com/latest/are-biofuels-and-e-fuels-the-only-sustainable-solution-to-power-our-existing-fleet-of-internal-combustion-engines/ (accessed Sep. 30, 2022).

[26] "The Opportunity For Sustainable Fuels In High-Performance Engines - Coryton." https://coryton.com/latest/the-opportunity-for-sustainable-fuels-in-high-performance-engines/ (accessed Sep. 30, 2022).

[27] A. Kar *et al.*, "Assessing the Impact of Lubricant and Fuel Composition on LSPI and Emissions in a Turbocharged Gasoline Direct

Injection Engine," *SAE Tech. Pap.*, vol. 2020-April, no. April, 2020, doi: 10.4271/2020-01-0610.

Contact Information

Contact details for the main author should be included here. Details may include mailing address, email address, and/or telephone number (whichever is deemed appropriate).

Acknowledgments

If the Acknowledgments section is not wanted, delete this heading and text.

Definitions/Abbreviations

SA	sample abbreviations
UBT	Use borderless table ≤ 3.5 inches wide.
test vector	Don't capitalise term unless an acronym or proper noun.

Appendix

The Appendix is one-column. If you have an appendix in your document, you will need to insert a continuous page break and set the columns to one. If you do not have an appendix in your document, this paragraph can be ignored and the heading and section break deleted.